

## Trends in the Electrochemical Polarization Potentiodynamic Reactivation Method – EPR

V. Číhal, S. Lasek, M. Blahetová, E. Kalabisová,\* and Z. Krhutová

VŠB – Technical University Ostrava, 17. listopadu 15, CZ 708 33, Ostrava,  
vladimir.cihal@vsb.cz, stanislav.lasek@vsb.cz, marie.blahetova@vsb.cz,  
zdenka.krhutova@vsb.cz

\*SVUOM Ltd. Praha, V Šáreckém údolí 2329, CZ 164 00, Praha 6,  
kalabisova@svuom.cz

Review

Received: October 9, 2006

Accepted: December 13, 2006

This method designed to examine the susceptibility to nonuniform corrosion, ranks among the more successful technique developments. One of its numerous advantages is that it allows nondestructive, on-site examination. EPR measurements are used to establish the resistance of stainless steels and alloys to intergranular corrosion and stress corrosion cracking *e.g.* in nuclear engineering applications as well as to study grain boundary precipitation and other minute local changes in alloy composition and structure.

By the EPR test, the specimen and/or the field object (working electrode) is tested in acid solutions, most often in solutions of sulfuric acid ( $c = 0.01\text{--}5 \text{ mol dm}^{-3} \text{ H}_2\text{SO}_4$ ) and potassium thiocyanate ( $c = 0.001 \text{ to } 0.1 \text{ mol dm}^{-3} \text{ KSCN}$ ). The principle of the measurements is to reactivate the sample from the incomplete passivity region. This indicates local changes in chemical composition in relation to phase transformations.

*Key words:*

Nonuniform corrosion, intergranular corrosion, stress corrosion, EPR method

### Introduction

The development of electrochemical potentiodynamic methods, from its early phases to its latest advances, has been applied to intergranular corrosion (IGC), stress corrosion cracking (SCC), pitting and crevice corrosion tests of stainless steels and other alloys and to the examination of their structure and properties. In assessing the susceptibility to intergranular and pitting corrosion by potentiodynamic polarization tests, the polarization curves which apply to the bulk of the alloy grains (the matrix) must be distinguished from those pertaining to grain boundaries.

The EPR test, using the double and/or single loop polarization is the preferred technique to establish the resistance of stainless steels and alloys to intergranular corrosion. EPR offers the advantage of rapidity and responds to the combined effects of a number of factors which influence the properties of materials, such as the effects of chromium-rich and molybdenum-rich carbides or phases, titanium carbides/sulfides and sulfide inclusions, in addition to the chromium/molybdenum depletion effect.

Measurements involving reactivation from a state of incomplete passivity indicate local changes in chemical composition, which relate *e.g.* to phase transformations in martensite-austenite steels. The electrochemical potentiodynamic tests are sensitive

enough to detect structural changes in heat treated or thermally influenced materials ranging far beyond stainless steels alone, and can be used for non-destructive testing aimed at elucidating the properties and behavior of materials.

### EPR history and principles

The electrochemical polarization techniques using solid electrodes represent a follow-up to the analytical methods which made use of the mercury drop electrode. Fundamentals including Heyrovsky's polarography,<sup>1</sup> Hickling's early potentiostat<sup>2</sup> and Pourbaix's thermodynamics of dilute aqueous solutions<sup>3</sup> were the launching pad for this new generation of measurements based on potentiostatic and potentiodynamic polarization. Used by numerous authors over the years<sup>4–10</sup> mainly to examine stainless steels, the polarization methods found their pinnacle in electrochemical potentiodynamic reactivation – the EPR test. From the Číhal's basis,<sup>11</sup> EPR came as a response to a situation in corrosion testing where a better, quantitative method was needed to measure the degree of sensitization (DOS) in welded components. Also, EPR was rapid, nondestructive and – when fully developed – well-suited for *in-situ* field measurements. Therefore, it came to enjoy worldwide acceptance, as documented by

the geographic spread of the major papers devoted to this topic.<sup>11–18</sup>

The principle of EPR is to measure the current generated in response to a uniform sweep of applied potential and to evaluate the characteristic features on the potential–current curve obtained.

In the single-loop EPR test (SL EPR) the polarization curve measured is a ‘reverse’ curve, with the potential scan from positive to negative, *i.e.* a sweep in the direction from a potential in or beyond the passive range to the open-circuit potential. In the double-loop EPR test (DL EPR) this is a cyclic curve consisting of a forward scan followed by a reverse scan, possibly with a delay at vertex which generally is located within the passive range or in the transpassive region.

The potentiodynamic polarization curves incorporate information not only on general corrosion but also on grain boundary depletion of chromium – and thus, on the susceptibility to intergranular attack as well as on changes of the metal structure. The polarization curve recorded for a sensitized steel specimen represents the sum of the curves for the chromium depleted and intact solid solutions. Two partial curves would be required to reflect the shares of total metal surface taken up by the two respective zones. This consideration also applies to the reactivation *i.e.* reverse curve, although the manifestations of the depleted regions differ depending on whether the potential is increasing or decreasing. The extent of depletion in chromium and, consequently, the degree of sensitization to intergranular corrosion can only be judged by resorting to comparative measurements capable of rendering the retardation of the total activation due to the formation of a passive film. Due to contact with a suitable electrolyte at an externally applied potential, a passive layer is formed on the alloy surface, its character depending chiefly on the composition of the basic solid solution of the alloy and on the electrolyte chemistry, and to a lesser extent on the mechanical stresses developed around the precipitated phases.

The potentiodynamic method of examining the susceptibility of stainless steels and alloys to intergranular corrosion issues from the principle of reactivation of a previously passive metal, the amount of reactivation depending on the chromium content in the solid solution. The method therefore points to the main cause underlying the intergranular corrosion of stainless steels – the depletion of chromium, which occurs due to the precipitation of complex chromium carbides.

Due to previous sensitizing exposure at elevated temperatures the chromium depleted grain boundaries are covered with a passive film at poten-

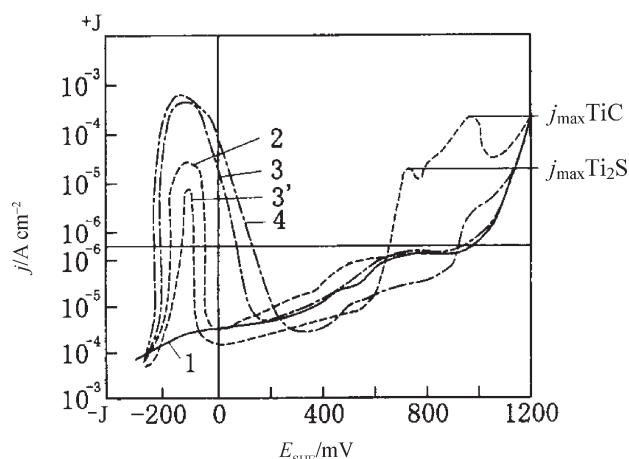


Fig. 1 – Potentiodynamic polarization curves; reverse sweep from transpassivity, for low carbon stainless steel ( $\alpha = 0.025\%$  C, 12.4 % Ni, 18.5 % Cr – curves 1,2,3) and for stabilized stainless steel (0.06 C, 12.05 Ni, 18.0 Cr, 0.65 Ti – curves 3', 4) in  $2.5 \text{ mol dm}^{-3} \text{ H}_2\text{SO}_4$  at  $70^\circ\text{C}$  ( $\text{N}_2$ ), scan rate  $\nu = 9 \text{ V h}^{-1}$  (UNIEUX, France 1969) after thermal treatment  
 1  $1150^\circ\text{C}/20'/\text{water} + 650^\circ\text{C}/1 \text{ h}/\text{water}$   
 2  $1150^\circ\text{C}/20'/\text{water} + 550^\circ\text{C}/20 \text{ h}/\text{water}$   
 3,3'  $1150^\circ\text{C}/20'/\text{water} + 550^\circ\text{C}/200 \text{ h}/\text{water}$   
 4  $1300^\circ\text{C}/20'/\text{water} + 550^\circ\text{C}/200\text{h}/\text{water}$

tials within the passive range. The passive film, however, is not perfect. On shifting the potential to the active region the passive film tends to preferentially redissolve at film defect sites which are activated first, whereas the film formed atop a sufficiently chromium-rich solid solution need not be disturbed at all under suitably selected conditions, or else its dissolution will manifest itself in only a small proportion on the over-all polarization curve. Thanks to this retardation of over-all corrosion during such reactivation the examiner has an opportunity to detect the nonuniform corrosion attack as revealed by the characteristic features of the curve. In EPR measurements, the active peak current, the ratio of active peak currents and/or charges on the forward and reverse scans, the reactivation charge, or some other parameters relating to the hysteresis in the active region is the evaluated response.

In order to express these relations quantitatively the retarded over-all corrosion of the surface initially covered with a largely intact or partially damaged passive film (represented by the reverse curve) is compared with the corrosion of the initially bare alloy surface (represented by the forward curve starting from the hydrogen evolution region).

## Experimental

Once again, the essence of the electrochemical potentiodynamic polarization methods is the rendering of the functional dependence of current density in response to changes of applied potential.

In the potentiodynamic reactivation test, the polarization curves are recorded under experimental conditions so selected as to bring to prominence any differences in electrochemical behavior of the chromium-depleted grain boundaries and the bulk of the material, *i.e.* the grains themselves, which have been produced by variations in chemical composition and/or structure.

The electrochemical polarization measurements are conducted using a potentiostat. The system operates with three electrodes of which one is the material being tested, another is a counter electrode and the third is a reference electrode. The corrosion current passes between the test specimen and the counter electrode, and responds to controlled changes of potential. Recommendation by SVÚOM Prague<sup>12</sup> is to apply DL EPR in  $c = 0.5\text{--}2.5 \text{ mol dm}^{-3} \text{ H}_2\text{SO}_4 + 0.01 \text{ mol dm}^{-3} \text{ KSCN}$  at ambient temperature in air, at a scan rate of  $9 \text{ V h}^{-1}$ . This allows both to examine changes if any in the specimen surface and to evaluate the sensitivity to intergranular corrosion to a sufficient accuracy (Fig. 2).

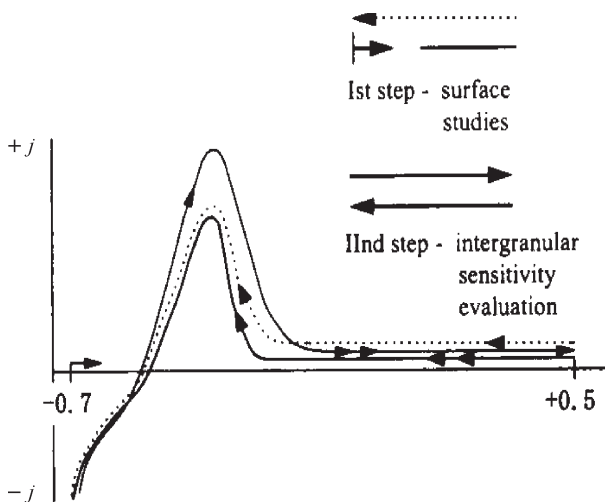


Fig. 2 – Double loop polarization reactivation measurement recommended by SVÚOM, Prague in  $0.5\text{--}2 \text{ mol dm}^{-3} \text{ H}_2\text{SO}_4 + 0.001 \text{ \% KSCN}$  at ambient temperature. The first step is employed particularly for surface studies and the second step for exact evaluation of intergranular corrosion sensitivity. Example of sensitized steel  $0.5\text{Cr}18\text{Ni}9$  in  $2 \text{ mol dm}^{-3} \text{ H}_2\text{SO}_4 + 0.01 \text{ \% KSCN}$  at ambient temperature, scan rate  $v = 9 \text{ V h}^{-1}$  (air), potential vs. SCE

### Material groups tested

Today's application range of EPR encompasses four prominent groups of materials: (i) general purpose commercial austenitic stainless steels; (ii) ferritic, martensitic and duplex stainless steels; (iii) nuclear grade and other heavy-duty steels; and (iv) nickel base alloys. The major cases are outlined below.

### Austenitic stainless steels

The EPR test is particularly well adapted to testing the susceptibility to intergranular corrosion (IGC) in general purpose Cr18Ni10 stainless steels but can also assist in studies of other materials and other forms of nonuniform corrosion. Indeed, the technique has had impact on pitting and crevice corrosion measurements as well as knife-line attack and stress corrosion cracking studies. It has also been very useful in the examination of structures and phases. Here we cannot devote more space to the most common type of steels since this would be to the detriment of the other corrosion resistant materials which, although less common, are the preferred choice for high duty applications where the knowledge that can be derived from the EPR measurements is the most critical. The wide interest in this technique has been evident from the massive body of publications over the last three decades. A comprehensive review detailing the individual results until 2004 has been presented elsewhere.<sup>13</sup>

The sensitization phenomenon is often responsible for intergranular stress corrosion cracking failures encountered in BWR primary water recirculation pipelines and in vessel components (Fig. 3).<sup>14–18</sup> Double loop EPR testing (in  $c = 0.5 \text{ mol dm}^{-3} \text{ H}_2\text{SO}_4 + 0.01 \text{ mol dm}^{-3} \text{ KSCN}$  solution at  $25 \text{ }^\circ\text{C}$ , at  $100 \text{ mV/min}$ ) confirmed that significant differences in the degree of sensitization developed in cast and wrought stainless steel structures after hot isostatic pressing when annealed at  $T = 675 \text{ }^\circ\text{C}$ . Electrochemical polarization can be efficacious in studies of thermal aging degradation of low-carbon, high-alloy stainless steels, such as Cr12Mn10Ni12Mo5N or Cr24Mn4Ni15N. Here it can detect microstructural changes, identify precipitates (such as  $\text{M}_{23}\text{C}_6$  car-

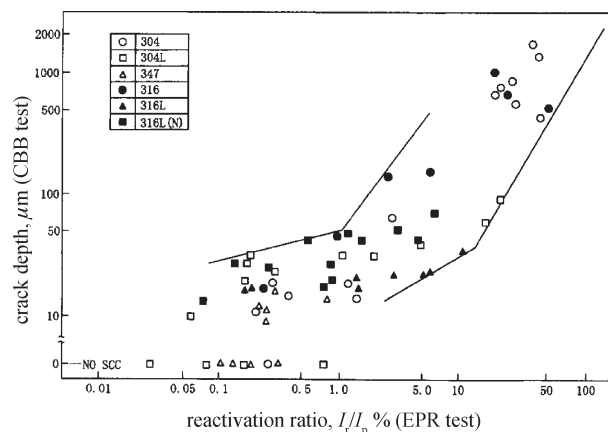


Fig. 3 – Correlation between reactivation ratio from the EPR test and SCC susceptibility from the CBB test of austenitic stainless steels. The  $I_r/I_p$  parameter was established from the EPR test carried out in  $0.5 \text{ mol dm}^{-3} \text{ H}_2\text{SO}_4 + 0.01 \text{ \% KSCN}$ , within the range of  $E_{\text{SCE}} = -450 \text{ to } +350 \text{ mV}$ , at a scan rate  $v = 100 \text{ mV min}^{-1}$ ; the CBB test was carried out at  $350 \text{ }^\circ\text{C}$ ,  $40 \text{ kgf cm}^{-2}$ ,  $\chi = 20 \cdot 10^{-6} \text{ Cl}^-$ ,  $\chi = 100 \cdot 10^{-6} \text{ O}_2$ ,  $\text{pH } 5.6\text{--}6.0$ .

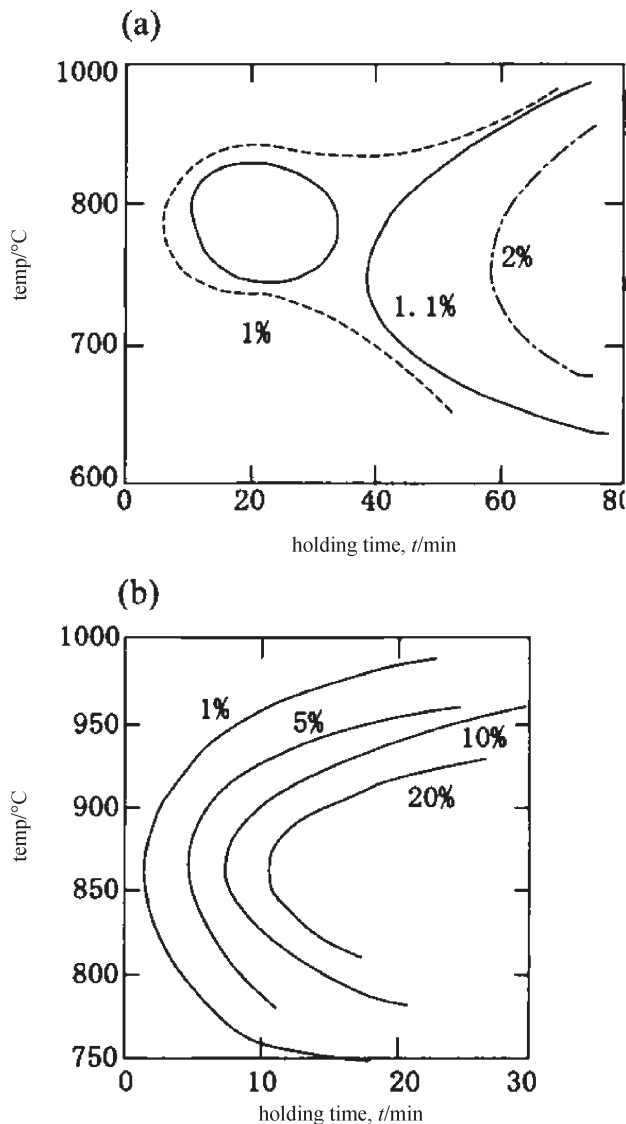


Fig. 4 – The time-temperature-sensitization diagram based on double loop EPR reactivation ratios for (a) 01Cr20Ni18Mo6CuN0.20 and (b) 01Cr24Ni22Mo7CuN0.53. The EPR test was carried out in 5 % HCl at 50 °C up to  $E_{sce} = 0.5$  V at a scan rate  $v = 6$  V h<sup>-1</sup>, reactivation coulombic charge ratio  $Q_i/Q_p$  in %.

bides, Laves phases and the  $\sigma$ -phase) and estimate the extent of precipitation.

Recently, high-nitrogen austenitic stainless steel containing up to 0.5 % N such as Cr24Ni15N are receiving increased attention. They offer strength advantages in nuclear fusion reactor applications. However, they are susceptible to Cr<sub>2</sub>N precipitation during thermal exposure at 550–800 °C (Fig. 4).<sup>19</sup>

#### Ferritic, martensitic and austeno-martensitic steels

Ferritic stainless steels such as Cr18Mo2 and Cr26Mo even if stabilized by titanium succumb to intergranular attack in oxidizing environments. Precipitation of carbides and nitrides cannot be avoided in low-interstitial ferritic Cr-Mo steels

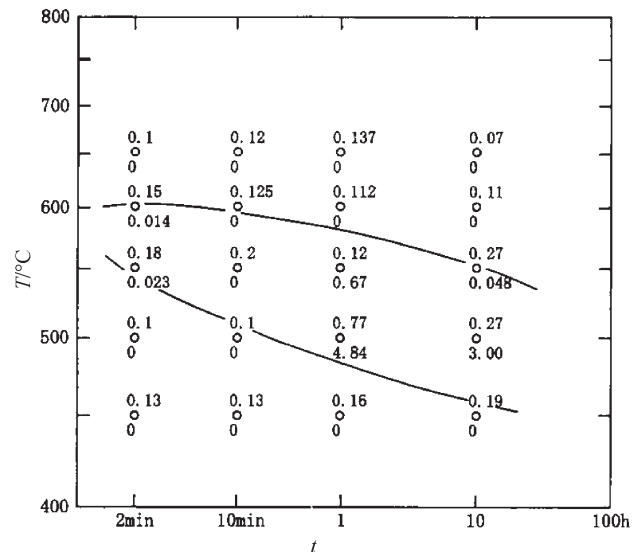


Fig. 5 – The susceptibility of 01Cr26Mo steel to intergranular corrosion related to temperature and annealing time. The upper values are the average corrosion rates (in g/m<sup>2</sup> · h) for 3 · 48 h cycles testing in boiling 65 % HNO<sub>3</sub>. The lower values (in mC cm<sup>-2</sup>) are taken from potentiodynamic reactivation measured in 2.5 mol dm<sup>-3</sup> H<sub>2</sub>SO<sub>4</sub> at 40 °C in nitrogen atmosphere. After initial heat treatment at 900 °C/30 min/water the steel shows a corrosion rate of 0.08–0.11 g m<sup>-2</sup> · h and a zero reactivation charge (0.0 mC cm<sup>-2</sup>).

( $\chi_{C+N} < 0.01$  %) during welding and heat treatment in the critical range of temperatures (Fig. 5). Type Cr29Ni2Mo4 steel can accommodate  $\chi = 0.02$  % nitrogen when welded.

Penetration of intergranular attack along the austenite grains produced by tempering has been demonstrated by EPR measurements in Cr17Ni2 martensitic steel (Fig. 6). Out of the many aspects

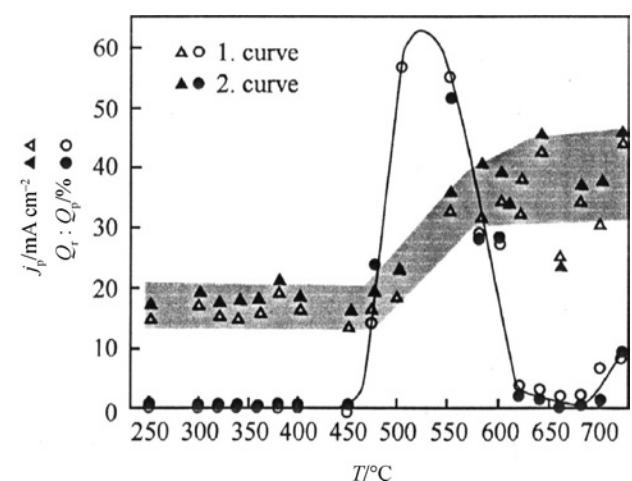


Fig. 6 – Effect of the tempering temperature on the critical passivation current density  $j_p$  and the  $Q_i/Q_p$  ratio of quenched-and-tempered martensitic 15Cr17Ni2 stainless steel (quenched at 1040°/ 3 min/oil and tempered for 4 h) as revealed by EPR measurements conducted in 0.5 mol dm<sup>-3</sup> H<sub>2</sub>SO<sub>4</sub> + 0.01 % KSCN at ambient temperature, at a scan rate  $v = 15$  V h<sup>-1</sup>.

deserving an in-depth discussion, the case of martensitic stainless steels such as Cr17Ni2, Cr16Ni2Mo and Cr16Ni3Mo is mentioned here to demonstrate the importance of making the right choice of EPR parameters to be evaluated when conducting sensitization tests. The critical passivation current density is not specific of chromium depletion alone, since it also reflects the general heterogeneity of structure. Consequently, the  $j_p$  readings when plotted against sensitization temperature tend to grow higher throughout the entire range. In contrast, the coulombic charge ratios on reactivation,  $Q_r/Q_p$ , show clearly defined peaks reflecting the maximum sensitization of grain boundaries. The shifts in annealing temperature corresponding to these peaks are due to compositional changes of the steels (e.g. the presence of Mo).

Molybdenum alloyed austeno-martensitic steels Cr13Ni6Mo and Cr14Ni4Mo may suffer IGC (Fig. 7). The same is true of low-carbon martensitic grades.<sup>20</sup> On the reverse scan begun at a potential affording an incomplete passivity, the reactivation peak is split (Fig. 8); the first peak corresponds to dissolution of the martensite matrix, whereas the peak occurring at a more positive potential is linked with the dissolution of a nickel-rich phase – either stable austenite or the product of its reverse transformation to martensite after tempering.

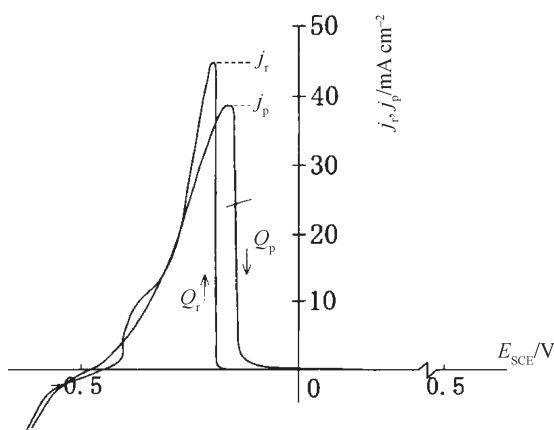


Fig. 7 – The potentiokinetic polarization curves of the martensite-austenite steel 03Cr13Ni6Mo, quenched from 800 °C and tempered at 500 °C; the EPR test was carried out in 0.5 mol dm<sup>-3</sup> H<sub>2</sub>SO<sub>4</sub> + 0.01 % KSCN at ambient temperature, within the range of -0.7/+0.5/-0.7V, at a scan rate  $\nu = 9 \text{ V h}^{-1}$ .

### Austeno-ferritic stainless steels

In strongly oxidizing media, austeno-ferritic duplex stainless steels such as Cr22Ni6Mo3N suffer preferential attack of  $\delta$ -ferrite. Degradation in thermally aged duplex steels Cr21Ni8 and Cr21Ni9Mo has also been studied by EPR. In duplex steels, EPR can be used to study the decomposition of fer-

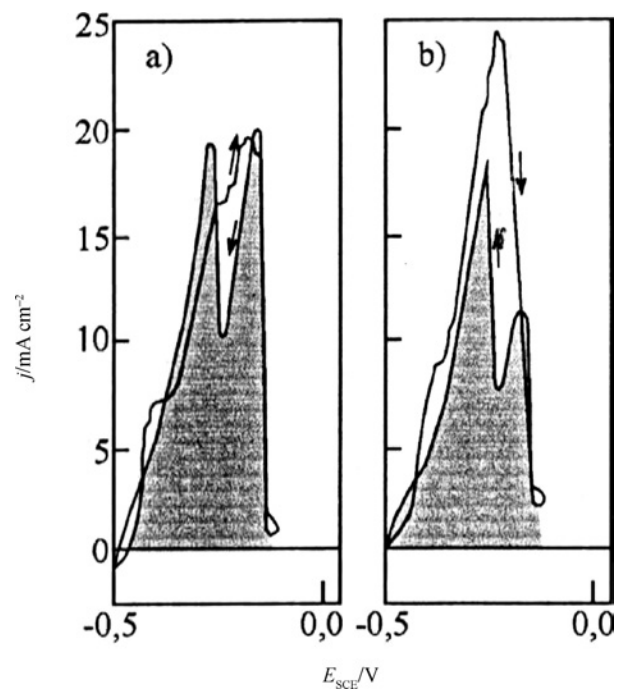


Fig. 8 – Potentiokinetic polarization curves of steel 03Cr13Ni6Mo in 0.5 mol dm<sup>-3</sup> H<sub>2</sub>SO<sub>4</sub> + 0.01 % KSCN at 25 °, scan rate 9 V h<sup>-1</sup> (start/end potential  $E_{SCE} = -0.7 \text{ V}$ , vertex potential  $E_{SCE} = -0.1 \text{ V}$ ) tempered after quenching at 1050 °C/2 h/air. a) tempered at 625°C / 6 h/air b) tempered at 575°C / 6 h/air

rite to e.g. the  $\sigma$ -phase and the  $\chi$ -phase, as well as the precipitation of carbides. Secondary phases have a large effect on the results obtained by EPR and, conversely, EPR can be used to examine secondary phases (Fig. 9).<sup>21–24</sup>

When using EPR to investigate structural components and changes, e.g. ferrite, the  $\sigma$ -phase, certain carbides, nitrides, sulfides, etc., a metallographic or other microscopic examination of the intergranular attack and the etched phases is recommended.

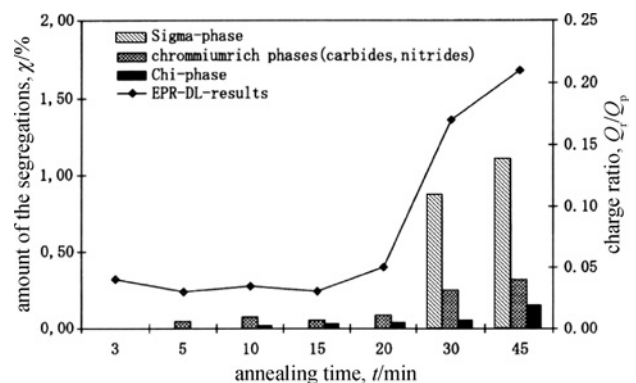


Fig. 9 – Relationship between the amount of segregation and the results of double loop EPR (charge ratio values) for type X2CrNiMoN22-5-3 duplex stainless steel after annealing at 750 °C. The EPR test in 0.5 mol dm<sup>-3</sup> H<sub>2</sub>SO<sub>4</sub> + 0.001 mol dm<sup>-3</sup> KSCN was run at potentials from  $E_{SCE} = -500$  to +200 mV and back to -500 mV at a scan rate  $\nu = 1 \text{ mV sec}^{-1}$ .

### Nickel base alloys

Prominent nickel alloys tested by EPR include Ni31Cr21Fe46 (Sanicro 31H), Ni33Cr21TiAl (Alloy 800), Ni74Cr16Fe9 (Inconel 600), NiCr30Fe (Alloy 690), Ni73Cr16Fe6TiAl (Inconel X-750), or Ni57Cr22Mo13W3Co (Alloy 22) etc., some of them used for nuclear waste containers.<sup>25</sup> Other nickel base and nickel-chromium alloys were of course also tested. It is an established fact that alloy composition has a strong effect on the dissolution rates even though sensitization may lead to similar depletion in chromium. High nickel alloys will not passivate as readily as iron base alloys but DL EPR can cope with this problem. In analogy to common stainless steels, EPR may be used to assess the susceptibility to IGC in these alloys.

Low temperature sensitization of Cr21Ni33TiAl (Alloy 800H), detected by DL EPR, was related to chromium depletion at grain boundaries (Table 1). This is of practical importance in screening the resistance to IGC and IGSCC of chemical furnace materials exposed to high service temperatures while in contact with a chemical product.<sup>26</sup>

The double loop electrochemical potentiokinetic reactivation test of Alloy 800 and/or Alloy 600 – widely used for steam generator tubing of nuclear power plants because of its favorable mechanical and corrosion properties at high temperatures, in spite of numerous cases being reported of IGC and IGSCC during normal operation – brought evidence of a beneficial effect of laser surface melting

of the alloy on its resistance to both these kinds of attack.<sup>27</sup> DL-EPR measurements conducted on Alloy 600 were highly discriminating and correlated well with IGSCC susceptibilities determined in deaerated Na<sub>2</sub>S<sub>4</sub>O<sub>6</sub> solution under deformation.

All this testing is of utmost importance to the nuclear industry. This is highlighted by the recent series of serious corrosion related problems experienced in nuclear power installations in various countries. For example, DL EPR tests confirmed that steam generator bolts made of Fe41Ni35Cr15W5TiAl alloy developed IGC susceptibility after a number of years in service. In other countries there also were numerous IGC and/or IGSCC related problems in power stations employing both PWR and BWR reactors, particularly where welded joints developed intergranular fissures.

### Low alloy steels

On the low-alloy side, in-service degradation and creep life of low-alloy (Cr2Mo1) steel is an example of using EPR to detect sensitization provoked by selective dissolution of M<sub>6</sub>C carbides. Numerous on-site measurements were also carried out in fossil fuel fired boilers.<sup>28</sup>

In the EPR test, the polarization curves are recorded under experimental conditions described in pertinent standards.<sup>29–33</sup> They should always be so selected as to bring to prominence any differences in electrochemical behavior of the chromium-de-

Table 1 – Results of DL EPR measurements of 0.2Cr21Ni33TiAl after prolonged exposure to temperatures of 450 °C and 650 °C and/or after subsequent heat treatment

Heat treatment	$j_p$ mA.cm <sup>-2</sup>	$j_r$ mA.cm <sup>-2</sup>	$Q_p$ C.cm <sup>-2</sup>	$Q_r$ C.cm <sup>-2</sup>	$Q_r/Q_p$
450 °C/30.000 h/air	56.0	26.00	2.222	1.210	54.4
1050 °C/2h/water (A)	49.0	0.04	2.036	0.000	0.0
(A) + 870 °C/3h/air	53.0	0.20	2.162	0.000	0.0
(A) + *	52.0	12.80	2.122	0.594	27.9
Heat treatment	$j_p$ mA.cm <sup>-2</sup>	$j_r$ mA.cm <sup>-2</sup>	$Q_p$ C.cm <sup>-2</sup>	$Q_r$ C.cm <sup>-2</sup>	$Q_r/Q_p$
650 °C/30.000 h/air	65.0	6.0	2.466	0.212	8.5
1050 °C/2h/water (A)	54.0	3.8	3.018	0.144	4.7
(A) + 870 °C/3h/air	53.0	0.4	2.300	0.004	0.2
(A) + *	50.5	18.0	2.162	0.852	39.4

\* = 800 °C/3h/ → 650 °C/4 h/ → 500 °C/air

pleted grain boundaries and the bulk of the material e.g. the grains themselves, which have been produced by variations in chemical composition and/or structure.

## Conclusion

The EPR test remains the most sensitive electrochemical testing technique in detecting the degree of sensitization. Its indications of IGC and IGSCC susceptibility correlate with information derived from microstructural examination.

The EPR tests have been applied to a variety of materials which include stainless steels of various types (austenitic, ferritic, martensitic and austeno-ferritic), nickel base alloys, special high-alloy stainless steels, and plain-carbon and low-alloy steels. However, the general-purpose austenitic stainless steels constitute the largest group of materials to which EPR tests have been applied. While the major stimulus for development of the EPR test came from the nuclear power industry, its use has been extended to the fossil fuels power industry, chemical industry, food and pharmaceutical industries, and many other industries employing steels and nickel base alloys.

Future developments in the EPR tests are expected to further extend its use as a nondestructive, *in-situ* test. The use of gel electrolytes is expected to facilitate its common use as an *in-situ* test. New parameters are being examined to fully take into account that the reactivation current comes mainly from the chromium-depleted regions. Potentially, EPR could be used to indirectly measure, on a macro scale, the minimum levels of chromium in the depleted regions of sensitized stainless steels and nickel base alloys. While the 1980s had seen major advances toward the formulation of commonly acceptable test conditions for stainless steels, the 1990s saw the same for nickel base alloys and also witnessed the development of a deeper understanding of the processes occurring during EPR. It is expected that the first decade of the millennium would witness a common acceptance of the test conditions for stainless steels and nickel base alloys and of the parameters describing the results of the EPR tests, facilitating formulation of common EPR test standards.

## ACKNOWLEDGEMENT

*This work was supported by the Czech Republic Grant Agency under projects Nos. 106/04/1272, 106/06/1621 and by the Czech Ministry of Education research program MSM 2579478701.*

## List of symbols

$c$	– concentration, mol dm <sup>-3</sup>
$E$	– potential, mV, V
$I$	– current, mA
$j$	– current density, mA cm <sup>-2</sup>
$Q$	– surface charge density, C cm <sup>-2</sup>
$T$	– temperature, °C
$t$	– time, min
$\chi$	– mole fraction, %
$\nu$	– potential scan rate, mV s <sup>-1</sup>

## References

1. Heyrovský, J., Research with the dropping mercury cathode. Part I – General Introduction. *Recueil des travaux chimiques, The Netherlands* **44** (1925) 488; Heyrovský, J., Shikata, M., Part II – The polarograph. **44** (1925) 496, 591.
2. Hickling, A., Wiring diagram of the potentiostat for chemical analysis of the solid electrode, *Trans. Faraday Soc.* **38** (1942) No.1, 27.
3. Pourbaix, M., *Thermodynamics of dilute aqueous solutions*, Edward Arnold Ed., London 1949.
4. Edeleanu, C., Method for the study of corrosion phenomena, *Nature* **173** (1954) 739; Corrosion control by anodic protection, *Metallurgia* **40** (1954) No. 2, 113.
5. Edeleanu, C., The potentiostat as a metallographic tool. *J. Iron Steel Inst.* **185** (1957) 482–8; **188** (1958) 122.
6. Clerbois, L., Clerbois, V., Massart, J., Intergranular corrosion of austenitic stainless steels (in French: Corrosion intercrystalline des aciers inoxydables austénitiques), *Electrochim. Acta* **1** (1959) 70–82.
7. Pražák, M., Pražák, V., Číhal, V., On the structure of the passive film on chromium steels (in German: Über den Aufbau der Passivschicht auf Chromstählen), *Z. Elektrochemie* **62** (1958) 739
8. Pražák, M., Číhal, V., Holinka, M., On the differentiation of phases in the structure by metallographic etching (in Czech: O diferenciaci strukturních fází při metalografickém leptění), *Chem. listy* **52** (1958) 1093; see also: *Coll. Czechoslov. Chem. Commun.* **24** (1959) 9.
9. Číhal, V., Pražák, M., Contribution to the explanation of intergranular corrosion of chromium-nickel steels (in Czech: Příspěvek k vysvětlení mezikrystalové koroze chromniklových ocelí), *Hutn. listy* **13** (1958) 496; see also: *Werkstoffe u. Korrosion* **9** (1958) 517; extended transl., *Corrosion (NACE)* **16** (1960) 530t–532t.
10. Číhal, V., Pražák, M., Potentiostat in metallography (in Czech: Potenciostat v metalografii), *Hutn. listy* **13** (1958) 496; see also: *J. Iron Steel Inst.* **193** (1959) 360.
11. Environmental degradation of material in nuclear power systems-water reactors, Breckenridge, Colorado, USA; *NACE TMS*, 1, 529–40, 1995.
12. Číhal, V., Desestret, A., Froment, M., Wagner, G.H., Étude de nouveaux tests potentiocinétiques de corrosion intergranulaire des aciers inoxydables. Étude CETIM, Centre de Recherches de Firminy, C. A. F. L., Rapport N° 958, 1969.
13. Číhal, V., Kubelka, J., EPR-Double Loop Recommendation of the State Research Institute for Materials Protection, SVÚOM Prague (1974).
14. Číhal, V., Shoji, T., Kain, V., Watanabe, Y., Štefec, R., Electrochemical Potentiokinetic Reactivation Technique, EPR – A Comprehensive Review. *Fracture & Reliability Re-*

- search Institute, Graduate School of Engineering, Tohoku University, Japan 2004
15. Clarke, W. L., Cowan, R. L., Walker, W. I. Detection of sensitization in stainless steel using electrochemical techniques, General Electric, report for US-NRC, CEAP 21382 and NUREG-0251-1, 1976.
  16. Clarke, W. L., The EPR method for the detection of sensitization in stainless steels, General Electric Co. report No. NUREG/CR-1095, GEAP-24888, R-5, San Jose, Calif., 1981, p. 85.
  17. Symp., Umemura, F., Akashi, M., Kawamoto, T., Evaluation of IGSCC susceptibility of austenitic stainless steels using electrochemical reactivation method (In Japanese.) *Boshoku Gijutsu (Corrosion Engrg. Japan)* **29** (1980) 163–9  
Kilian, R., Bruemmer, G., Ilg, V., Meier, V., Teichmann, H., Wachter, O., Proc. 7th Int.
  18. Kondo, T., Kiuchi, K., Tsuji, H., Thermomechanical treatment of types 304 and 316 stainless steels-grain aging, recrystallizing process (SAR)-IGC and IGSCC immunization, Proc. Seminar on Countermeasures for pipe cracking in BWRs, EPRI WS-79-174, Palo Alto, Calif., Workshop report, Vol. 3, May 1980, paper no. 45, 1–15.
  19. Číhal, V., Klimsza, A., Lasek, S., Elaboration of the EPR method for the high-alloyed steels, Proc. EUROCORR'96, Nice, XP5, 1–4, 1996.
  20. Číhal, V., Hubáčková, J., Kubelka, J., Mazanec, K., The potential polarization method for the evaluation of martensite-austenite stainless steels, *Materials Chemistry & Physics*, **11** (1984) 279.
  21. Scully, J. R., Kelly, R. Q., An electrochemical test for detecting the intergranular corrosion susceptibility of a duplex stainless steel, *Corrosion (NACE)* **42** (1986) 537.
  22. Schultze, S., Selective Korrosion von Duplexstahl, Thesis, Faculty of Mechanical Engineering, Otto von Guericke University, Magdeburg, Germany 1999.
  23. Verneau, M., Audouard, J.-P., Charles, J., Properties and examples of practical applications of superduplex stainless steels, Proc. from 5<sup>th</sup> Duplex stainless steels conference, Oct. 21–23 (1997) Maastricht, The Netherlands, pp. 845–55.
  24. Merino, C., Pardo, A., Lopez, M. D., Advances en Ciencia y tecnologia del Acero Inoxydable, Eds. J. A. Adriozaola, J. Botella, Instituto Andaluz de Tecnologia, Sevilla, Spain, 2001, p. 15.
  25. Raja, K. S., Namjeski, S. A., Radmilović, V. T. A., Jones, D. A., Electrochemical methods to detect susceptibility of Ni-Cr-Mo-W alloy 22 to intergranular corrosion, *Metallurgical and Materials Trans. A*, **36A** (2005) 115.
  26. Wagner, G. H., The EPR technique to evaluate special questions on the corrosion resistance of high-alloyed materials (in German: Beurteilung spezieller Fragen zur Beständigkeit hochlegierter Werkstoffe mit dem EPR-Versuch – Cihal-Test), *Werkstoffe u. Korrosion* **52** (2001) 15.
  27. Ahemadabadi, P., Kain, V., Singh, P. R., De, P. K., *J. of Materials and Engineering Performance*, **12** (2003) 529.
  28. Shoji, T., Watanabe, Y., Yi, Y. S., Komazaki, S., Suggested procedures for electrochemical material characterisation, spec. reprint RIFT, Tohoku University, Sendai, Japan 1997.
  29. JIS G 0590 – 1986: Method of electrochemical potentiokinetic reactivation ratio measurement for stainless steels.
  30. GOST 9.914 – 1991: Ispitaniya na mezhkristallitnyu korroziyu 5. Metod potentsiodinamicheskoi reaktivatsii, p 12–15.
  31. ASTM G 1 08 – 1994: Test method for Electrochemical Potentiokinetic Reactivation (EPR) for detecting sensitization of AISI type 304 and 304L stainless steels.
  32. JIS G 0580:2003 (JSA): Method of electrochemical potentiokinetic reactivation ratio measurement for stainless steels, Ref. no. HS G 0580:2003 (E).
  33. ISO/DIS 12732: Method for electrochemical potentiokinetic reactivation test (based on Cihal's test).